JOURNAL OF VIROLOGY, Jan. 2009, p. 572–583 Vol. 83, No. 2
0022-538X/09/$08.00+0 doi:10.1128/JVI.01715-08
Copyright © 2009, American Society for Microbiology. All Rights Reserved.

Differential CD4$^+$ T-Lymphocyte Apoptosis and Bystander T-Cell Activation in Rhesus Macaques and Sooty Mangabeys during Acute Simian Immunodeficiency Virus Infection$^\nabla$

Mareike Meythaler,[1,4] Amanda Martinot,[2] Zichun Wang,[1] Sarah Pryputniewicz,[1] Melissa Kasheta,[1] Binhua Ling,[3] Preston A. Marx,[3] Shawn O'Neil,[2] and Amitinder Kaur[1]*

Divisions of Immunology[1] and Comparative Pathology,[2] New England Primate Research Center, Harvard Medical School, One Pine Hill Drive, Southborough, Massachusetts 01772; Division of Microbiology, Tulane National Primate Research Center, Covington, Louisiana 70433[3]; and Institut für Klinische und Molekulare Virologie, Friedrich-Alexander-Universität Erlangen-Nürnberg, Schlossgarten 4, 91054 Erlangen, Germany[4]

Received 12 August 2008/Accepted 23 October 2008

In contrast to pathogenic lentiviral infections, chronic simian immunodeficiency virus (SIV) infection in its natural host is characterized by a lack of increased immune activation and apoptosis. To determine whether these differences are species specific and predicted by the early host response to SIV in primary infection, we longitudinally examined T-lymphocyte apoptosis, immune activation, and the SIV-specific cellular immune response in experimentally infected rhesus macaques (RM) and sooty mangabeys (SM) with controlled or uncontrolled SIV infection. SIVsmE041, a primary SIVsm isolate, reproduced set-point viremia levels of natural SIV infection in SM but was controlled in RM, while SIVmac239 replicated to high levels in RM. Following SIV infection, increased CD8$^+$ T-lymphocyte apoptosis, temporally coinciding with onset of SIV-specific cellular immunity, and elevated plasma Th1 cytokine and gamma interferon-induced chemokine levels were common to both SM and RM. Different from SM, SIV-infected RM showed a significantly higher frequency of peripheral blood activated CD8$^+$ T lymphocytes despite comparable magnitude of the SIV-specific gamma interferon enzyme-linked immunospot response. Furthermore, an increase in CD4$^+$ and CD4$^-$CD8$^-$ T-lymphocyte apoptosis and plasma tumor necrosis factor-related apoptosis-inducing ligand were observed only in RM and occurred in both controlled SIVsmE041 and uncontrolled SIVmac239 infection. These data suggest that the "excess" activated T lymphocytes in RM soon after SIV infection are predominantly of non-virus-specific bystander origin. Thus, species-specific differences in the early innate immune response appear to be an important factor contributing to differential immune activation in natural and nonnatural hosts of SIV infection.

Sooty mangabeys (*Cercocebus atys*) (SM) are African Old World primates that are natural hosts of the simian immunodeficiency virus (SIV) and rarely progress to AIDS (21, 30). Even though SIV infection of SM shares important similarities with pathogenic lentiviral infection, including the presence of persistent moderate to high-level SIV viremia, there is a striking absence of increased lymphocyte turnover, increased immune activation, and increased apoptosis during the chronic phase of SIV infection (2, 17, 30, 31). The mechanisms underlying this difference remain unclear.

Induction of apoptosis in early SIV infection has been shown to be a predictor of later disease progression in SIV-infected rhesus macaques (RM) (24, 32). Only a limited number of studies have compared apoptosis in natural and nonnatural hosts during the acute phase of SIV infection. In studies with African green monkeys (AGM), lymph node (LN) apoptosis in the first 8 weeks after SIV infection was reported to be of limited magnitude compared to that in RM (5). Whether these differences are related to the innate or virus-specific host response is not known. In this study, we examined the kinetics of T-lymphocyte apoptosis and its relationship to viral load, immune activation, and the SIV-specific cellular immune response in experimentally SIV-infected SM and RM in the setting of uncontrolled and controlled infection. SIVsmE041 infection reproduced the set-point viremia levels of natural infection in SM but was controlled in RM, while SIVmac239 infection resulted in high-level viremia in RM. Our data show that an acute increase in apoptosis and activation of CD8$^+$ T lymphocytes temporally coinciding with the onset of a cellular immune response to SIV were common features of SIV infection in all three experimental settings. However, an acute increase in peripheral blood CD4$^+$ T-lymphocyte apoptosis and activation, along with increased plasma tumor necrosis factor-related apoptosis-inducing ligand (TRAIL) levels, was observed only in RM and occurred in both controlled and uncontrolled SIV infection. Differences in the magnitude of T-lymphocyte activation but not the anti-SIV gamma interferon (IFN-γ)-secreting T-lymphocyte response in RM and SM indicate the possibility of a larger pool of bystander activated T lymphocytes expanding during acute SIV infection in RM. These data suggest that species-specific differences in the innate host response contribute to the divergent outcome of SIV infection in RM and SM.

* Corresponding author: Mailing address: Division of Immunology, New England Primate Research Center, Harvard Medical School, One Pine Hill Drive, Southborough, MA 01772. Phone: (508)-624-8169. Fax: (508)-624-8172. E-mail: amitinder_kaur@hms.harvard.edu.

$^\nabla$ Published ahead of print on 5 November 2008.

MATERIALS AND METHODS

Animals. SM were housed at the Yerkes National Primate Research Center, Atlanta, GA, while RM were housed at the New England Primate Research Center (NEPRC), Southborough, MA. Four SIV-negative SM and 10 SIV-negative RM were enrolled in the present study. All animals were maintained in accordance with institutional and federal guidelines for animal care (26).

SIV infection. The primary isolate SIVsmE041, derived from a naturally SIV-infected SM that developed AIDS (21), and the pathogenic molecular clone SIVmac239 (provided by Ron Desrosiers, NEPRC) were used for SIV infection studies. Experimental SIVsmE041 infection was performed by intravenous inoculation of 1 ml plasma ($n = 2$ SM) or 25 ng p27 equivalent of SIVsmE041 virus stock grown on peripheral blood mononuclear cells (PBMC) of SIV-negative SM ($n = 2$ SM and 4 RM). The pathogenic molecular clone SIVmac239 (3,000 50% tissue culture infective doses [$TCID_{50}$]) was used to infect six SIV-negative RM via the intrarectal route.

Sample collection and processing. Blood from SM was collected in heparin Vacutainer tubes and heparin CPT Vacutainer tubes (Becton Dickinson Vacutainer Systems, Franklin Lakes, NJ), shipped on ice, and processed the next day at NEPRC. Blood collected from RM housed at NEPRC was subjected to a similar overnight delay before processing. Lymphocytes isolated by density gradient centrifugation (Lymphocyte Separation Medium; MP Biomedicals Inc., Solon, OH) from heparin blood were used for apoptosis studies and phenotyping. Enzyme-linked immunospot (ELISPOT) assays were performed on PBMC isolated from heparin CPT tubes that had been centrifuged at $950 \times g$ for 30 min within 1 hour of blood collection.

LN biopsy tissue collected in RPMI 1640 medium (Cellgro, Herndon, VA) supplemented with 10% fetal calf serum (Sigma-Aldrich, St. Louis, MO), 2 mM L-glutamine (Cellgro), 50 IU/ml penicillin (Cellgro), 50 μg/ml streptomycin (Cellgro), and 10 mM HEPES buffer (Cellgro) (R-10 medium) was mechanically dissected and homogenized using sterile techniques. Lymphocytes were separated from cell debris by straining through a 70-μm cell strainer (BD Biosciences, San Jose, CA) and used for flow cytometry or ELISPOT assays. Plasma was collected from blood in heparin Vacutainer tubes by centrifugation for 10 min at $950 \times g$ the day after collection and was used for enzyme-linked immunosorbent assay (ELISA) and cytometric bead array.

Antibodies and immunophenotyping. Fluorochrome-conjugated antibodies of anti-human specificity were obtained from BD Biosciences Pharmingen (San Jose, CA) unless stated otherwise. These included anti-CD3 (clone SP34-2)–allophycocyanin (APC) or –APC-Cy7; anti-CD4 (clone L200)–APC, –phycoerythrin (PE), –peridinin chlorophyll protein (PerCP), or –peridinin chlorophyll protein cychrome 5.5; anti-CD8 (clone SK1)–PerCP; anti-CD8 (clone RPA-T8)–Alexa700; anti-active caspase-3 (clone C92-605)–fluorescein isothiocyanate (FITC) or –PE; and anti-Ki67 (clone B56)–FITC. Streptavidin-APC and Q-dot655 (Invitrogen) were used as secondary reagents to detect biotinylated primary antibodies. For compensation settings anti-mouse immunoglobulin (Ig), κ/Negative Control Compensation Particles (BD Biosciences) were used. Four-color and polychromatic flow cytometry was used for immunophenotyping. Samples were run on a FACSCalibur or LSR II (BD Biosciences), and at least 200,000 events were acquired. Data were analyzed using FlowJo software 8.7.3. (Tree Star, Inc., San Carlos, CA).

Detection of apoptosis. The anti-active caspase-3 monoclonal antibody (MAb) was used for flow cytometric detection of apoptosis in isolated lymphocytes that were fixed and permeabilized using commercial fixation and permeabilization reagents (Caltag Laboratories, Burlingame, CA) as previously described (33). Apoptosis was measured ex vivo in freshly isolated peripheral blood and LN lymphocytes that were not subjected to prior stimulation or culture in medium. Isotype and fluorescent minus one controls were included as negative controls to validate the caspase-3 staining. In all instances, cells induced to undergo apoptosis by 5 μM camptothecin or 10 μM dexamethasone (Sigma-Aldrich) for 18 h were used as postive controls. T-lymphocyte apoptosis was also measured in fixed LN tissue sections by active caspase-3 immunohistochemistry (IHC) as described previously (28). Briefly, IHC for cleaved caspase-3 and CD20 were performed sequentially on the same sections of formalin-fixed, paraffin-embedded LN. Tissue sections were deparaffinized in xylene and rehydrated through graded ethanol solutions to distilled water. Endogenous peroxidase activity was blocked by incubation in 3% H_2O_2, and antigen retrieval was accomplished by microwaving sections for 20 min in citrate buffer (Dako Corp., Carpinteria, CA). Tissue sections were treated for nonspecific protein binding (Protein Block; Dako) and then sequentially incubated for 30 min at room temperature with polyclonal rabbit anti-human cleaved caspase-3 (Cell Signaling Technology, Inc., Boston, MA) followed by biotinylated goat anti-rabbit IgG. Antigen-antibody complexes were localized by application of streptavidin-peroxidase conjugate (Dako) followed by development in the chromogenic substrate 3,3′-diaminobenzidine (Dako). To detect CD20 expression, endogenous alkaline phosphatase activity was blocked in 5 mM levamisole before tissue sections were incubated overnight at 4°C with mouse anti-human CD20 (clone L26; Dako). The next day, tissues were incubated with biotinylated horse anti-mouse IgG, followed sequentially by alkaline phosphatase-conjugated streptavidin and the alkaline phosphatase substrate Vector Blue (Vector Labs, Burlingame, CA).

The extent of programmed cell death in paracortical T lymphocytes was estimated by counting the number of caspase-3^+ $CD20^-$ cells within CD20-negative paracortical regions and dividing by the total area of the LN section, expressed as cells/mm^2. LN images were captured using an Optronics DEI-750 charge-coupled device camera (Meyer Instruments, Inc., Houston, TX) mounted on an Olympus AH-2 microscope (Olympus America, Inc., Center Valley, PA), and computer image quantification of LN area (in mm^2) was accomplished using Leica QWin software (Leica Microsystems, Inc., Bannockburn, IL), as described elsewhere (28).

Plasma SIV RNA. The concentrations of SIVsmE041 and SIVmac239 RNA in plasma were determined as previously described (3, 33). Briefly, blood was collected in tubes containing the anticoagulant EDTA and centrifuged at $1,200 \times g$ for 10 min within 3 h of collection. Removed plasma was centrifuged again at $1,200 \times g$ for 10 min, and aliquots of cell-free plasma were stored at −80°C. Plasma RNA was extracted with the QIAamp viral RNA kit (Qiagen), and SIV RNA was measured by real-time reverse transcriptase PCR (7700 Sequence Detection System; PE Applied Biosystems). Random hexamers were used to prime reverse transcription. Primers and probe targeting a highly conserved region in the 5′ untranslated region (SIVsmE041) or SIV *gag* (SIVmac239) were used, and the SIV RNA copy number was determined by interpolation onto a standard curve of viral RNA standards.

ELISPOT assay. IFN-γ ELISPOT assays were performed against peptide pools spanning the SIV proteome as previously described (33). Overlapping peptides were based on the sequence of SIVmac239 and consisted of 15-amino-acid-long peptides overlapped by 11 amino acids. Ten SIV peptide pools, each representing one SIV protein (exception two pools for Pol), were used for stimulation and measurement of the total SIV-specific response. Peptides were used at a final concentration of 1 to 2 μg/ml, with the dimethyl sulfoxide concentration being maintained at <0.5% in all functional assays. The capture- and biotinylated-detector-matched MAb pair for IFN-γ were clones GZ-4 and 7-B6-1 (Mabtech, Nack Strand, Sweden), respectively. Briefly, sterile 96-well polyvinylidene difluoride MultiScreen-IP plates (Millipore, Bedford, Mass.) coated with anticytokine MAb were plated with unfractionated PBMC at 200,000 to 300,000 cells/well for SIV-specific stimulation. Stimulation of 100,000 cells with staphylococcal enterotoxin B (100 ng/ml; Sigma-Aldrich) was used as a positive control, while stimulation with medium alone was used as a negative control. After overnight stimulation at 37°C in a 5% CO_2 incubator, cells were removed by extensive washing and incubated for 2 h at room temperature with biotinylated detector MAb. Spots were developed by successive incubation with streptavidin-alkaline phosphatase followed by the substrate nitroblue tetrazolium/5-bromo-4-chloro-3-indolylphosphate (NBT/BCIP) buffer (Moss, Inc., Pasadena, MD). Spots were counted on a KS ELISPOT automated reader system (Carl Zeiss, Inc., Thornwood, NY) using KS ELISPOT 4.2 software (performed by ZellNet Consulting, Inc., Fort Lee, NJ). Frequencies of responding cells obtained after subtracting background spots in negative control wells were expressed as spot-forming cells (SFC) per million PBMC. ELISPOT responses to individual SIV proteins that were more than twofold above those of negative control wells and greater than two standard deviations above the mean in SIV-seronegative monkeys were considered positive.

ELISA. IFN-α and soluble TRAIL levels were measured in plasma using the commercial available IFN-α (PBL Biomedical Laboratories, Piscataway, NJ) and TRAIL (Biosource, Carlsbad, CA) ELISA kits. Typically, samples were run in duplicates in at least two independent experiments.

Cytometric bead array. Plasma cytokine and chemokine levels were measured by the cytometric bead array as per the manufacturer's protocol using the Th1/Th2 nonhuman primate kit and chemokine kit (BD Biosciences). Briefly, 50 μl of the mixed capture beads, 50 μl of the standards or test samples, and 50 μl of the PE detection reagent were added to the assay tubes and incubated for 3 hours at room temperature in the dark. Thereafter, assay tubes were washed with 1 ml wash buffer, fixed with 2% paraformaldehyde for 30 min at room temperature, and resuspended in 100 to 200 μl wash buffer. Samples were run on a FACSCalibur, which was set up using the cytometer setup beads as described in the manual. Typically, samples were run in duplicates in at least two independent experiments.

ISH analysis. Productively infected SIV-positive cells were identified by in situ hybridization (ISH) for SIV RNA in LN tissue as described previously (27, 28),

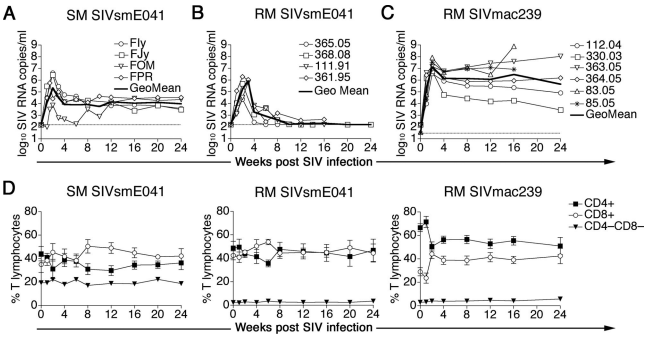

FIG. 1. Kinetics of plasma SIV viremia and peripheral T-lymphocyte counts in experimentally infected SM and RM. (A to C) Plasma SIV RNA in four SIVsmE041-infected SM (A), four SIVsmE041-infected RM (B), and six SIVmac239-infected RM (C). SIVsmE041 was inoculated intravenously as 25 ng p27 equivalent of virus stock (FIy, FJy, and all four RM) or 1 ml plasma from SM E041 (FOM and FPR). SIVmac239 (3,000 $TCID_{50}$) was inoculated intrarectally. The geometric mean of plasma SIV RNA for each group is represented by the solid black line. The detection limit (160 copies/ml for SIVsmE041 and 30 copies/ml for SIVmac239) is denoted by the dotted line. (D) Changes in frequency of T-lymphocyte subsets during acute SIV infection. Means and standard errors of the means for SIVsmE041-infected SM (left panel), SIVsmE041-infected RM (middle panel), and SIVmac239-infected RM (right panel) are shown.

using digoxigenin-labeled antisense riboprobes (Lofstrand Labs, Gaithersburg, MD) spanning the entire genomes of either the SIVsmmPGm5.3 molecular clone of SIVsmFGb for SIVsmmE041-infected SM and RM or SIVmac239 for SIVmac239-infected RM. After hybridization, sections were washed extensively and bound probe was detected by IHC, using alkaline phosphatase-conjugated sheep antidigoxigenin F(ab) fragments (Roche) and the chromogen NBT/BCIP (Roche). Sections were counterstained with nuclear fast red (Vector Labs, Burlingame, CA).

Statistical analysis. Comparisons between groups or between time points were performed with the two-tailed unpaired and paired *t* tests, respectively. Correlation analysis was performed with the Pearson test. All statistical analysis was performed using the GraphPad Prism software version 4.0c (GraphPad Software, Inc., La Jolla, CA).

RESULTS

Differential replication of SIVsmE041 in RM and SM. In this study we used the primary SIVsm isolate SIVsmE041 (21) for experimental infection to compare differences in immune events and apoptosis during acute SIV infection in SM and RM. Previously we had shown that experimental SIVmac239 infection of SM was not representative of natural SIV infection, since it did not lead to sustained viremia in chronic infection (18). Since SIVsmE041 had not been passaged in RM, we reasoned that it was more likely to reproduce the viral replication patterns of natural SIV infection in SM.

Initially, two SIV-negative SM (FOM and FPR) were inoculated intravenously with plasma from the naturally SIV-infected SM E041 (Fig. 1A). Subsequently, virus stock of SIVsmE041 grown on PBMC of SIV-negative SM was obtained and used to inoculate two SIV-negative SM (FIy and FJy) and four RM (111.91, 361.95, 365.05, and 368.05) via the intravenous route (Fig. 1A and B). Additionally, six RM inoculated intrarectally with 3,000 $TCID_{50}$ of pathogenic SIV mac239 were also investigated (Fig. 1C).

SIVsmE041 infection of four SM resulted in arithmetic mean peak and set-point plasma SIV RNA levels of 1.8×10^6 and 1.6×10^4 copies/ml, respectively (Fig. 1A). The set-point viremia levels established in the SIVsmE041-infected SM were in the range observed in naturally SIV-infected SM (30, 31). In four RM infected with SIVsmE041, peak viremia levels (arithemetic mean, 7.7×10^5 copies/ml plasma SIV RNA) were comparable to those in SM, but plasma viremia was undetectable or <500 plasma SIV RNA copies/ml at the set point (Fig. 1B). Unlike SIVsmE041, the pathogenic molecular clone SIVmac239 replicated to high levels in six RM, with arithmetic mean peak and set-point viremia levels of 2.2×10^7 and 7.3×10^6 plasma SIV RNA copies/ml, respectively (Fig. 1C). The different viral replication patterns of SIVsmE041 and SIVmac239 infection in RM allowed comparison of early events during controlled or uncontrolled SIV infection in a pathogenic host as opposed to uncontrolled SIV infection in a natural host.

All three experimental groups showed a transient decline in peripheral blood total $CD4^+$ T-lymphocyte counts and a variable degree of $CD8^+$ T lymphocytosis in the first 8 weeks after SIV infection (Fig. 1D). The frequency of peripheral blood $CD4^+$ T lymphocytes recovered to near-baseline levels in the SIVsmE041-infected SM and RM but showed a persistent decline to roughly 60% of baseline levels in the SIVmac239-infected RM (Fig. 1D). Consistent with our previous findings, the baseline frequency of $CD4^-CD8^-$ double-negative T lymphocytes was significantly higher in SM than in RM (A. Kaur, unpublished data) and did not change after SIV infection (Fig. 1D). The majority of double-negative T lymphocytes in SM express the αβ T-cell receptor, and their function is being investigated (A. Kaur, unpublished data).

Differential ex vivo apoptosis of peripheral blood T-lymphocyte subsets during acute SIV infection in SM and RM. In chronic pathogenic human immunodeficiency virus (HIV) or SIV infection, increased lymphocyte apoptosis is evident only after in vitro culture in medium or after mitogen or T-cell receptor stimulation (7, 13, 23). In the few published comparative studies of apoptosis in natural and nonnatural hosts during acute SIV infection, apoptosis was examined in tissue sections by IHC or in lymphocytes by flow cytometry (5, 8, 29). In this study we investigated lymphocyte apoptosis ex vivo in freshly isolated peripheral blood and LN lymphocytes not subjected to prior culture or stimulation, using flow cytometric detection of intracellular active caspase-3 (Fig. 2A). Intracellular accumulation of active caspase-3 was validated as a marker of T-lymphocyte apoptosis by concurrent flow cytometric detection of cleaved poly(ADP-ribose) polymerase (PARP), an end product of the proteolytic action of active caspase-3 on its substrate PARP, as well as by terminal deoxynucleotidyltransferase-mediated dUTP-biotin nick end labeling (TUNEL). In two SIVmac239-infected macaques, cleaved PARP colocalized with active caspase-3, and the frequency of active caspase-3-positive T lymphocytes showed a strong positive correlation with TUNEL-positive T lymphocytes (data not shown).

Flow cytometric detection of ex vivo apoptosis in freshly isolated peripheral blood lymphocytes could be performed in two of the four SIVsmE041-infected SM and in all the SIV-infected RM (Fig. 2). A five- to sixfold increase in $CD8^+$ T-lymphocyte apoptosis, but a minimal to no increase in apoptosis of $CD4^+$ and double-negative ($CD4^-CD8^-$) T lym-

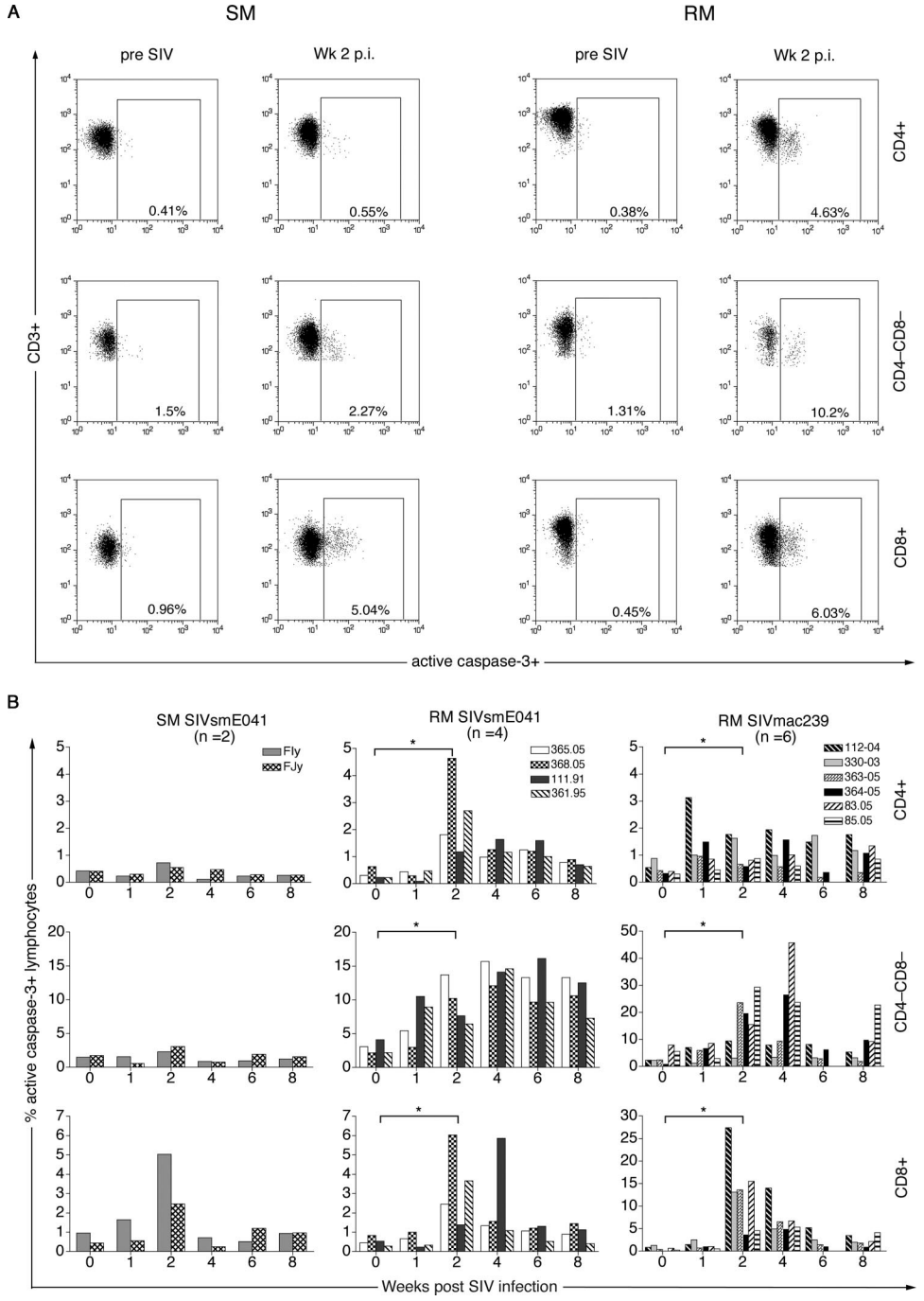

FIG. 2. Differential ex vivo T-lymphocyte apoptosis in peripheral blood in SM and RM following SIV infection. (A) Representative flow data of active caspase-3 staining of $CD4^+$ (top), $CD4^-CD8^-$ (middle), and $CD8^+$ (bottom) T lymphocytes before and after SIVsmE041 infection for one SM and one RM (B) Kinetics of active caspase-3 expression in peripheral $CD4^+$ (top), $CD4^-CD8^-$ (middle), and $CD8^+$ (bottom) T lymphocytes in two SIVsmE041-infected SM, four SIVsmE041-infected RM, and six SIVmac239-infected RM in the first 8 weeks after SIV infection. Data on individual animals in each group are shown. Asterisks denote P values of <0.05 for comparison between week 0 and week 2 time points determined by the two-tailed paired t test. p.i., postinfection.

phocytes, was observed in the two SIVsmE041-infected SM in the first 2 weeks following SIV infection (Fig. 2B). In contrast, a significant 2- to 36-fold increase in $CD4^+$, $CD4^-CD8^-$, and $CD8^+$ T-lymphocyte apoptosis was seen during this period in both SIVsmE041- and SIVmac239-infected RM and persisted above pre-SIV infection levels (Fig. 2B). The 3- to 13-fold increase in $CD8^+$ T-lymphocyte apoptosis in SIVsmE041-infected RM at 2 weeks after SIV infection was comparable in magnitude to that in the SIVsmE041-infected SM (Fig. 2B) but was of lower magnitude than that in SIVmac239-infected RM ($P = 0.055$; unpaired t test), suggesting that $CD8^+$ T-lymphocyte apoptosis was related to the extent of viral replication.

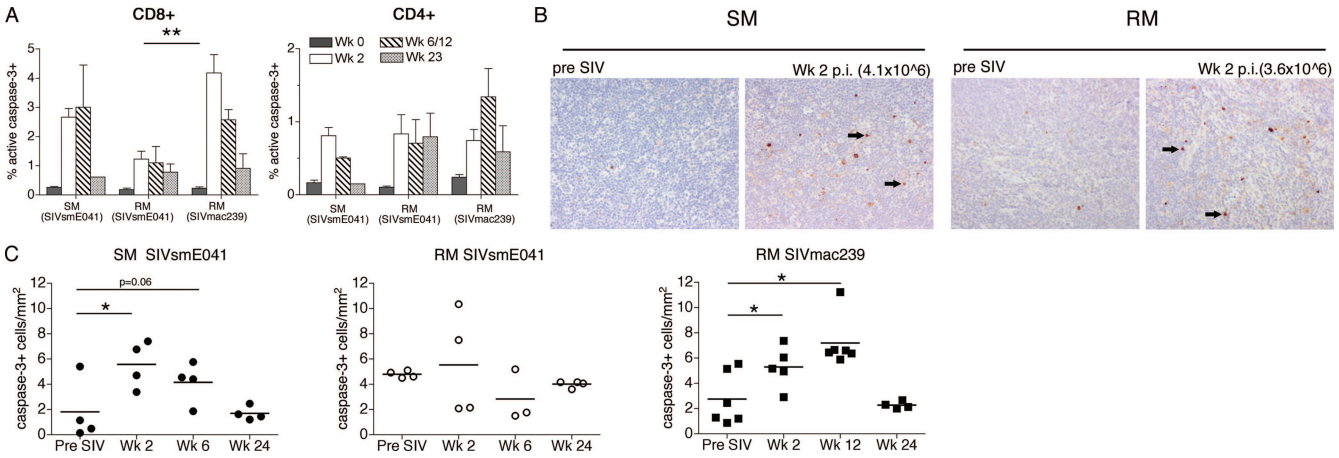

FIG. 3. T-lymphocyte apoptosis in peripheral LNs of SM and RM during acute SIV infection. (A) Percentage of active caspase-3-positive $CD4^+$ and $CD8^+$ T lymphocytes in LNs determined by flow cytometry. Means and standard errors of the means for SIVsmE041-infected SM ($n = 2$), SIVsmE041-infected RM ($n = 4$), and SIVmac239-infected RM ($n = 6$) shown. Asterisks denote P values of <0.01 as determined by the two-tailed unpaired t test. (B) Representative active caspase-3 IHC on LNs of one SIVsmE041-infected SM and one SIVmac239-infected RM before and 2 weeks after SIV infection. Caspase-3-positive cells (brown 3,3′-diaminobenzidine chromogen, indicated by the arrows) in the entire paracortical zone of the LN were counted and numbers were normalized relative to the entire LN section in mm^2. Plasma SIV RNA values are shown in parentheses. All sections are at a magnification of ×200 with hematoxylin counterstaining. (C) Absolute numbers of active caspase-3-positive T lymphocytes in LNs before and after SIV infection. Asterisks denotes P values of <0.05 as determined by the two-tailed paired t test.

Apart from the transient decline in $CD4^+$ T lymphocytes, detection of increased T-lymphocyte apoptosis was not temporally associated with detectable changes in the peripheral counts of T-lymphocyte subsets (Fig. 1D).

In contrast to $CD8^+$ T-lymphocyte apoptosis, the striking difference in $CD4^+$ and $CD4^-CD8^-$ T-lymphocyte apoptosis between SM and RM appeared to be species specific and independent of the extent of viral replication. SIVsmE041 replicated to comparable levels in SM and RM yet induced $CD4^+$ and $CD4^-CD8^-$ T-lymphocyte apoptosis only in RM. Conversely, despite a difference of more than 1 log in levels of peak viremia in SIVmac239- and SIVsmE041-infected RM, there was no significant difference in the magnitude of $CD4^+$ and $CD4^-CD8^-$ T-lymphocyte apoptosis between the two groups (Fig. 2B and data not shown).

Increased LN T-lymphocyte apoptosis is a feature of acute SIV infection in both SM and RM. In a recent study, serial IHC analysis of peripheral LN revealed increased apoptosis in RM but not AGM in acute SIV infection (5). In the current study, we investigated apoptosis of peripheral LN T lymphocytes by both flow-cytometric (Fig. 3A) and IHC (Fig. 3B and C) analyses of active caspase-3. As for peripheral blood, the frequency of ex vivo $CD4^+$ and $CD8^+$ T-lymphocyte apoptosis in freshly isolated LN lymphocytes could be examined in two of the four SIVsmE041-infected SM and in all the SIV-infected RM (Fig. 3A), while semiquantitative analysis of T-lymphocyte apoptosis in LN sections by IHC could be performed on all the SM and RM (Fig. 3B and C).

Similar to the case for peripheral blood, an increase in $CD8^+$ T-lymphocyte apoptosis was observed in both species (Fig. 3A). At 2 weeks after SIV infection, $CD8^+$ T-lymphocyte apoptosis in the SIVmac239-infected RM was of significantly greater magnitude than that of the SIVsmE041-infected RM (Fig. 3A). Different from the case for peripheral blood, a small increase in LN $CD4^+$ T-lymphocyte apoptosis ($<1\%$ apoptotic $CD4^+$ T lymphocytes) was observed in both SM and RM (Fig. 3A). Since the LN is an early site of SIV replication, the small increase in $CD4^+$ T-lymphocyte apoptosis in the LN but not peripheral blood of SIV-infected SM may reflect the presence of higher numbers of productively SIV-infected $CD4^+$ T lymphocytes in close proximity to uninfected $CD4^+$ T lymphocytes in the LN. It is likely that the difference in $CD4^+$ T-lymphocyte apoptosis between RM and SM is primarily due to lower or absent apoptosis of uninfected $CD4^+$ T lymphocytes in SM rather than due to differences in apoptosis of productively infected $CD4^+$ T lymphocytes. If so, it is perhaps not surprising that a high concentration of productively infected $CD4^+$ T lymphocytes at the peak of viral replication in the LN would manifest as increased $CD4^+$ T-lymphocyte apoptosis in the LNs of both species. The magnitude of acute $CD4^+$ T-lymphocyte apoptosis appeared to be similar in SM and RM, but by week 23, $CD4^+$ T-lymphocyte apoptosis had returned to baseline levels in the SM but not in the RM (Fig. 3A).

Semiquantitative analysis of apoptotic T lymphocytes in the LN paracortex by active caspase-3 IHC showed a significant and comparable increase in apoptosis in the T-cell zones of SIVsmE041-infected SM and SIVmac239-infected RM at 2 weeks after SIV infection (Fig. 3B and C). The frequency of productively SIV-infected cells in the LN paracortex at this time point was similar in SM and RM and did not correlate with the frequency of active caspase-3-positive cells in the paracortex (Fig. 4A and B). We also did not observe a correlation between plasma viremia and peripheral blood $CD4^+$ and $CD8^+$ T-lymphocyte apoptosis in acute SIV infection (Fig. 4C and D).

Relationship between $CD8^+$ T-lymphocyte apoptosis, $CD8^+$ T-lymphocyte activation, and the SIV-specific cellular immune response in acute SIV infection. Since primary viral infections are characterized by a rapid expansion of activated virus-specific $CD8^+$ T lymphocytes that later undergo apoptosis (25),

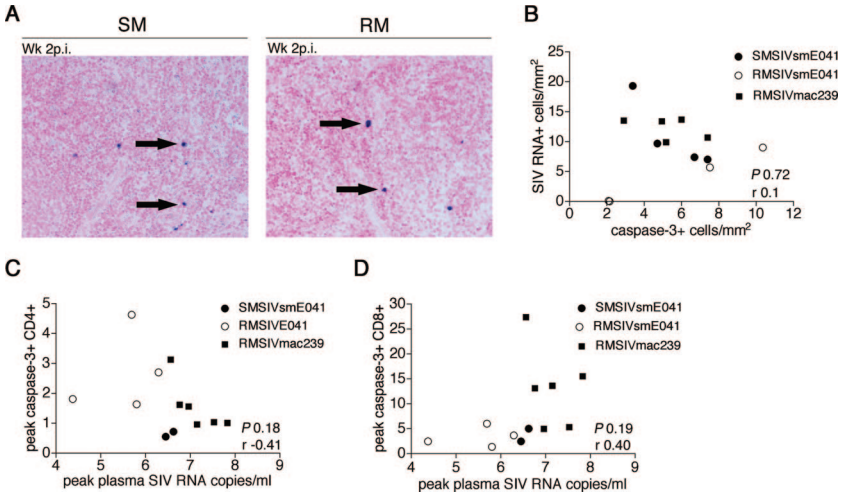

FIG. 4. Relationship between SIV load and T-lymphocyte apoptosis. (A) Representative SIV RNA ISH to detect productively infected cells (dark blue NBT/BCIP chromogen, as indicated by the arrows) in peripheral LNs. Week two data are shown for one SIVsmE041-infected SM (left) and one SIVmac239-infected RM (right). Magnification, ×200; nuclear fast red counterstain. (B) Relationship between number of SIV RNA-positive cells determined by ISH and number of active caspase-3-positive cells in the paracortical zone of the LN at 2 weeks postinfection. (C and D) Relationship between peak plasma SIV viremia and frequency of apoptotic $CD4^+$ (C) and apoptotic $CD8^+$ (D) T lymphocytes. Correlations were determined by the Pearson correlation test.

we investigated the relationship between $CD8^+$ T-lymphocyte apoptosis, $CD8^+$ T-lymphocyte activation, and the SIV-specific cellular immune response.

A significant increase in the frequency of peripheral blood Ki67-positive $CD8^+$ T lymphocytes was observed in both SM and RM between 2 and 4 weeks following SIV infection ($P < 0.05$; paired t test). However, the frequency of Ki67-positive $CD8^+$ T lymphocytes at peak and week 12 after SIV infection were significantly higher in RM than in SM (Fig. 5A). In contrast to $CD8^+$ T-lymphocyte activation, a significant increase in the frequency of circulating Ki67-positive $CD4^+$ T lymphocytes was only observed in the SIVsmE041- and SIVmac239-infected RM ($P < 0.05$; paired t test) in the first 4 weeks following SIV infection (Fig. 5B). At its peak, the frequency of Ki67-positive $CD4^+$ T lymphocytes in the SIV-infected RM was significantly higher than that the SIV-infected SM (Fig. 5B). Surprisingly, the frequency of Ki67-positive $CD4^+$ T lymphocytes in SIVmac239-infected RM was significantly lower than that in the SIVsmE041-infected SM early in SIV infection (Fig. 5B). The reason for this difference is not clear, although it may be related to a greater loss of activated $CD4^+$ T lymphocytes in SIVmac239-infected RM (Fig. 1D).

In both species, a significant direct correlation between the frequency of circulating Ki67-positive and active caspase-3-positive $CD8^+$ T lymphocytes was observed (Fig. 5C), suggesting the presence of activation-induced apoptosis following SIV infection. Consistent with the differential activation of peripheral blood $CD4^+$ and $CD8^+$ T lymphocytes in SM but not RM, a significant positive correlation between the frequency of Ki67-positive $CD4^+$ and $CD8^+$ T lymphocytes during acute SIV infection was observed in the two groups of RM but not in the SM (Fig. 5D). A significant direct correlation between Ki67-positive $CD4^+$ T lymphocytes and apoptotic $CD4^+$ T lymphocytes was observed in the two groups of SIV-infected RM but not in the SIV-infected SM (Fig. 5E).

To investigate the relationship between activation-induced apoptosis and SIV-specific cellular immunity in primary infection, IFN-γ ELISPOT responses toward the entire SIVmac239 proteome were monitored longitudinally (Fig. 6A). In both species, SIV-specific IFN-γ ELISPOT responses were detected 1 to 3 weeks after SIV infection and coincided temporally with the increase in frequency of Ki67-positive and active caspase-3-positive $CD8^+$ T lymphocytes (Fig. 6A). At 2 weeks after SIV infection, the total peripheral blood SIV-specific IFN-γ ELISPOT response ranged between 155 and 5,550 SFC/10^6 PBMC (mean, 2,373) in four SIVsmE041-infected RM, between 877 and 8,589 SFC/10^6 PBMC (mean, 3,702) in six SIVmac239-infected RM, and between 300 and 2,790 SFC/10^6 PBMC (mean, 1,077) in four SIVsmE041-infected SM (Fig. 6B). Since the peptides used for testing were based on the sequence of SIVmac239, it is possible that the measured SIV-specific ELISPOT responses, particularly against SIV Env and the accessory proteins, were underestimated in the SIVsmE041-infected SM and RM compared to the SIVmac239-infected RM. Even so, the magnitude of the measured total SIV-specific IFN-γ ELISPOT response in SIVsmE041-infected SM at 2 weeks after SIV infection did not differ significantly from that in either group of SIV-infected RM (Fig. 6B). At later time points in the peripheral blood, and at all time points in the LNs, there was no difference in the magnitude of the ELISPOT response between RM and SM (Fig. 6B and C). The comparable magnitude of SIV-specific cellular immune responses in SM and RM during acute SIV infection was similar to our previous findings for chronic SIV infection (33).

These data suggest that the higher frequency of activated $CD8^+$ T lymphocytes during acute SIV infection in RM is unlikely to be due to a stronger virus-specific T-lymphocyte response mounted by SIV-infected RM. Instead, the "excess" $Ki67^+$ $CD8^+$ T lymphocytes in RM early in SIV infection likely reflect higher numbers of non-SIV-specific "bystander" activated T cells in RM than in SM. Although the numbers are small, it is noteworthy that a trend for a positive correlation

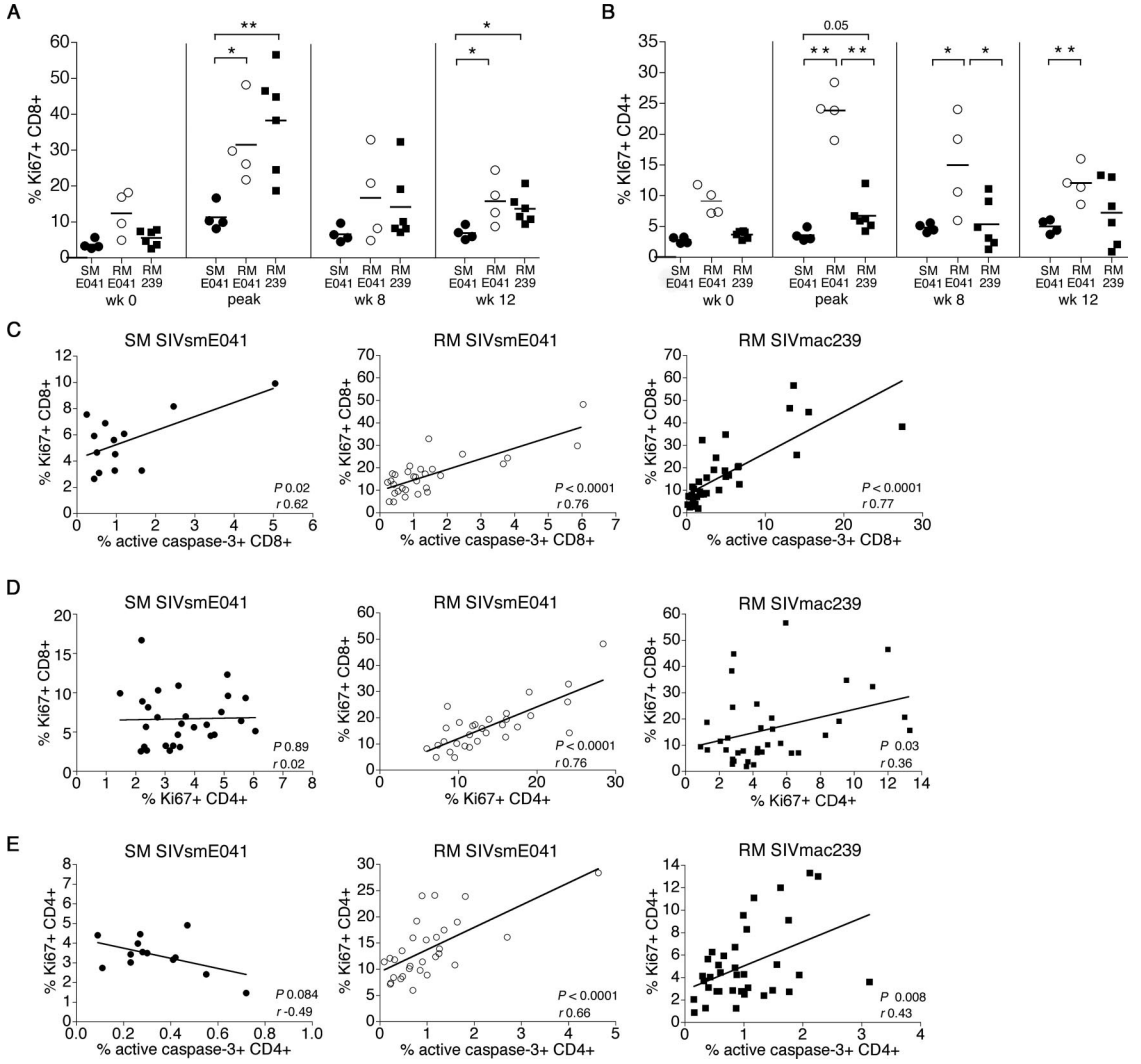

FIG. 5. Relationship between apoptosis and proliferation of peripheral $CD8^+$ and $CD4^+$ T lymphocytes in acute SIV infection. (A and B) Serial comparison of the frequency of Ki67-positive $CD8^+$ (A) and Ki67-positive $CD4^+$ (B) T lymphocytes in SIVsmE041-infected SM (closed circles), SIVsmE041-infected RM (open circles), and SIVmac239-infected RM (closed squares) prior to and following SIV infection. "Peak" refers to the time point (weeks 1 to 4) in individual animals when the maximal increase in $Ki67^+$ T lymphocytes was observed. Asterisks denote *P* values of <0.05 (*) and <0.01 (**) for difference between two groups using the two-tailed unpaired *t* test. (C) Correlation between Ki67-positive $CD8^+$ T lymphocytes and active caspase-3-positive $CD8^+$ T lymphocytes in the first 12 weeks following SIV infection in SIVsmE041-infected SM ($n = 2$; left), SIVsmE041-infected RM ($n = 4$; middle), and SIVmac239-infected RM ($n = 6$; right). (D) Correlation between $Ki67^+$ $CD8^+$ T lymphocytes and $Ki67^+$ $CD4^+$ T lymphocytes in the first 12 weeks following SIV infection in SIVsmE041-infected SM ($n = 4$; left), SIVsmE041-infected RM ($n = 4$; middle), and SIVmac239-infected RM ($n = 6$; right). (E) Correlation between Ki67-positive $CD4^+$ T lymphocytes and active caspase-3-positive $CD4^+$ T lymphocytes in the first 12 weeks following SIV infection in SIVsmE041-infected SM ($n = 2$; left), SIVsmE041-infected RM ($n = 4$; middle), and SIVmac239-infected RM ($n = 6$; right). Correlation coefficients (*r*) were determined by the Pearson correlation test.

between the frequency of Ki67-positive $CD8^+$ T lymphocytes and the magnitude of the SIV-specific IFN-γ ELISPOT response at 2 weeks after SIV infection was observed in the SM ($r = 0.94$; $P = 0.05$) but not in the RM ($r = 0.06$; $P = 0.86$).

Elevated plasma TRAIL in RM but not SM during acute SIV infection. Recent publications have implicated TRAIL in the pathogenesis of $CD4^+$ T-lymphocyte apoptosis in pathogenic SIV and HIV infection (14, 16, 19). To investigate the basis for differential $CD4^+$ T-lymphocyte apoptosis in SM and RM during acute SIV infection, we longitudinally monitored plasma levels of TRAIL and IFN-α, along with proinflammatory cytokines and chemokines.

Baseline levels of plasma TRAIL prior to SIV infection showed considerable variation between animals, ranging between 17.6 and 35.2 pg/ml in SM and between 0 and 59.8 pg/ml in RM (Fig. 7A). Following SIV infection, a significant increase in plasma TRAIL was observed in the SIVsmE041- and SIVmac239-infected RM but not in the SIVsmE041-infected SM (Fig. 7A). Irrespective of the pre-SIV infection levels, the magnitudes of increase in plasma TRAIL were comparable in the SIVsmE041- and SIVmac239-infected macaques. However, the kinetics of the increase was different in the two groups of SIV-infected RM. The maximal increase in plasma TRAIL was observed

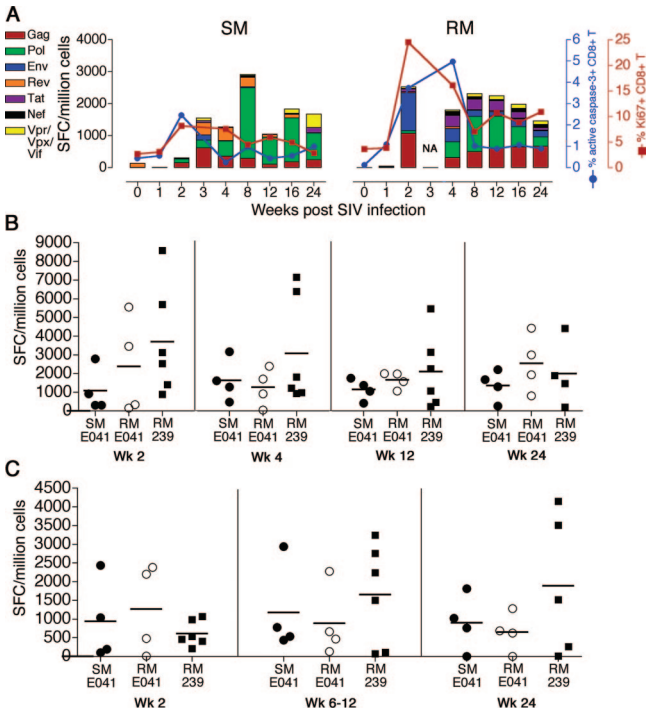

FIG. 6. Comparison of SIV-specific cellular immune responses in the acute phase of SIV infection in SM and RM. (A) Kinetics of peripheral blood SIV-specific IFN-γ ELISPOT responses in relation to the frequency of active caspase-3-positive (blue line) and Ki67-positive (red line) $CD8^+$ T lymphocytes for one SIVsmE041-infected SM (left) and one SIVmac239-infected RM (right). (B and C) Comparison of peripheral blood (B) and LN (C) SIV-specific IFN-γ ELISPOT responses in SIVsmE041-infected SM (closed circles), SIVsmE041-infected RM (open circles), and SIVmac239-infected RM (closed squares). The sum of the IFN-γ ELISPOT responses to all nine SIV proteins is shown.

as early as 1 week after SIV infection in five of six SIVmac239-infected RM, while it occurred at 2 to 4 weeks after SIV infection in the SIVsmE041-infected RM (Fig. 7A).

With the exception of three SIVmac239-infected RM, the increase in plasma TRAIL was not accompanied by an increase in plasma IFN-α levels that was detectable by ELISA (Fig. 7B), raising the possibility that IFN-α is not the only inducer of TRAIL in SIV-infected macaques. Although peak plasma levels of TRAIL and IFN-α showed a significant positive correlation in RM, it was largely due to detectable IFN-α levels in 3 of the 10 SIV-infected RM (Fig. 7C). A correlation between TRAIL and plasma viremia was not detected (data not shown). However, RM with peak plasma SIV RNA levels of $>10^{6.5}$ copies/ml had higher levels of plasma TRAIL and IFN-α than RM with lower peak viremia levels (Fig. 7D and E). Interestingly, plasma TRAIL levels in the first 12 weeks after SIV infection were directly correlated to the frequency of apoptotic $CD4^+$ but not $CD8^+$ T lymphocytes (Fig. 7F), suggesting that TRAIL-mediated apoptosis was one of the mechanisms contributing to the differential $CD4^+$ T-lymphocyte apoptosis in nonnatural and natural hosts of SIV infection.

Levels of plasma interleukin-2 (IL-2), IL-6, IFN-γ, MIG (CXCL9), monocyte chemoattractant protein 1 (MCP-1) (CCL2), and IP-10 (CXCL10) increased in the majority of animals in the first 2 weeks after SIV infection, while an increase in IL-8 and RANTES was observed only in the SIV-infected RM (Fig. 8). Changes in plasma cytokine and chemokine levels tended to be modest or absent in SIVsmE041-infected RM compared to SIVmac239-infected RM (Fig. 8), likely reflecting the lower viral loads in this group. With the exception of RANTES, the plasma levels of Th1 and proinflammatory cytokines and chemokines at 1 and 2 weeks after SIV infection did not differ in magnitude between SIVmac239-infected RM and SIVsmE041-infected SM (Table 1 and data not shown). Overall, the similarities in the acute proinflammatory cytokine and chemokine response to SIV in the two species suggest common pathways of activation of the innate immune system that are not involved in the pathogenesis of divergent T-lymphocyte activation during acute SIV infection.

DISCUSSION

In this study, the kinetic analysis of ex vivo T-lymphocyte apoptosis in relation to generalized immune activation and the virus-specific cellular immune response has provided novel insight into differences and similarities in the early host response to SIV infection in a natural host and a nonnatural host. Both SM and RM responded to SIV infection with the appearance of a virus-specific cellular immune response that coincided temporally with an acute increase in the frequency of circulating and LN $CD8^+$ T lymphocytes undergoing apoptosis and expressing the proliferation antigen Ki67, suggesting that initiation of the adaptive immune response was intact and comparable in both species. The quality of the early host response also appeared to be similar as evidenced by a comparable increase in plasma levels of Th1 cytokines and interferon-inducible chemokines in both species. Three striking features distinguished the early host response to SIV infection in RM and SM. (i) An increase in apoptosis of peripheral blood $CD4^+$ and double-negative T lymphocytes was observed only in the RM. (ii) A significant increase in plasma TRAIL was seen in the SIV-infected RM but not in the SIV-infected SM and was positively correlated with $CD4^+$ T-lymphocyte apoptosis. (iii) The circulating pool of proliferating, activated $CD4^+$ and $CD8^+$ T lymphocytes during the acute phase of SIV infection was significantly higher in RM than in SM despite comparable SIV-specific cellular immune responses. These differences were independent of the infecting SIV strain, peak viral replication, or extent of control of viremia and thus appeared to be species specific.

Comparative studies of apoptosis in natural and nonnatural hosts during acute SIV infection are limited and have been largely confined to IHC analysis of peripheral LNs (5, 8). A prospective study with SIV-infected AGM and RM did not detect increased T-lymphocyte apoptosis during acute infection in AGM (5). However, this study and another (8) observed an acute increase and a relatively rapid resolution of T-lymphocyte apoptosis in the LNs of SM during acute SIV infection, suggesting that the host response to SIV may differ with the natural host species. The current study is novel in several respects. In addition to LN IHC, the measurement of apoptosis in freshly isolated lymphocytes by flow cytometry allowed quantitative assessment of the ex vivo frequency of apoptotic cells in phenotypically defined T-lymphocyte subsets and re-

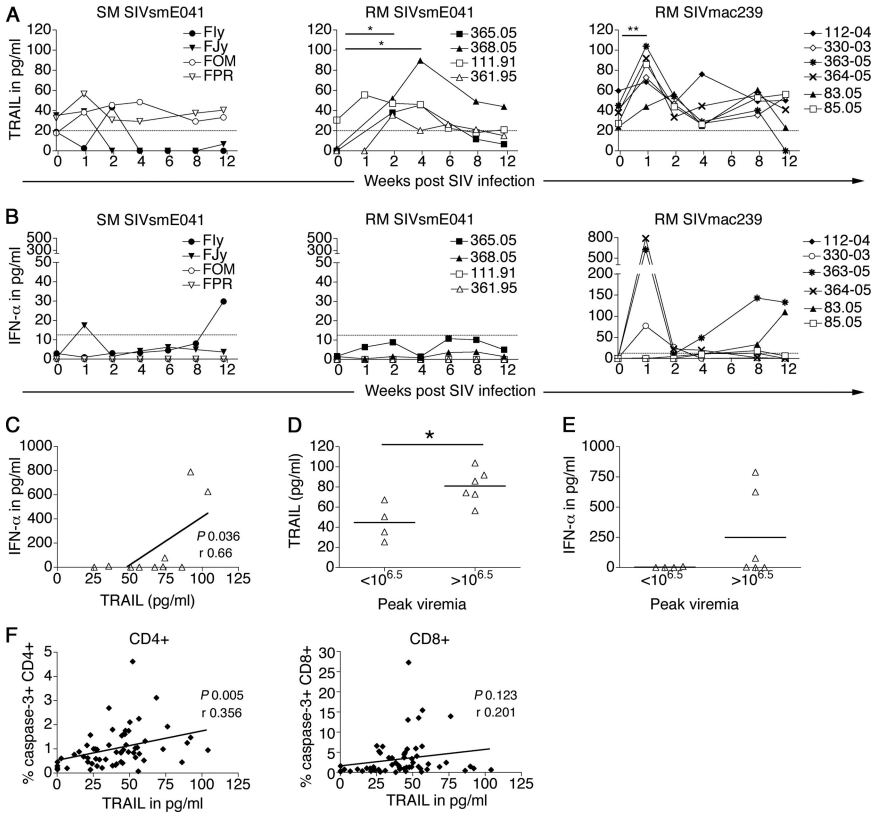

FIG. 7. Changes in plasma TRAIL and IFN-α levels during acute SIV infection. (A and B) Kinetic measurement of plasma TRAIL (A) and IFN-α (B) in four SIVsmE041-infected SM (left), four SIVsmE041-infected RM (middle), and six SIVmac239-infected RM (right) before and after SIV infection. Means of replicates from one representative experiment are shown. The limits of detection of ELISA (TRAIL, 20 pg/ml; IFN-α, 12.5 pg/ml) are indicated by the dotted lines. Asterisks denote P values of <0.05 (*) and <0.01 (**) as determined by the two-tailed paired t test. (C) Correlation of peak TRAIL and IFN-α levels. (D and E) Plasma levels of TRAIL (D) and IFN-α (E) in RM for animals with peak plasma SIV RNA levels lower or higher than $10^{6.5}$ copies/ml. The asterisk denotes a P value of <0.05 by the two-tailed unpaired t test. (F) Relationship between plasma TRAIL and frequencies of apoptotic $CD4^+$ T lymphocytes (left panel) and apoptotic $CD8^+$ T lymphocytes (right panel) in the first 12 weeks after SIV infection. Correlation coefficients (r) were determined by the Pearson correlation test.

vealed a hitherto-unreported early species-specific divergence in $CD4^+$ and double-negative, but not $CD8^+$, T-lymphocyte apoptosis in the peripheral blood of SM and RM following SIV infection. Increased activation and apoptosis of $CD4^+$ and double-negative T lymphocytes distinguished SIV-infected RM from SIV-infected SM as early as 1 week after SIV infection and was observed in the settings of both controlled and uncontrolled SIV infection in RM. These differences were

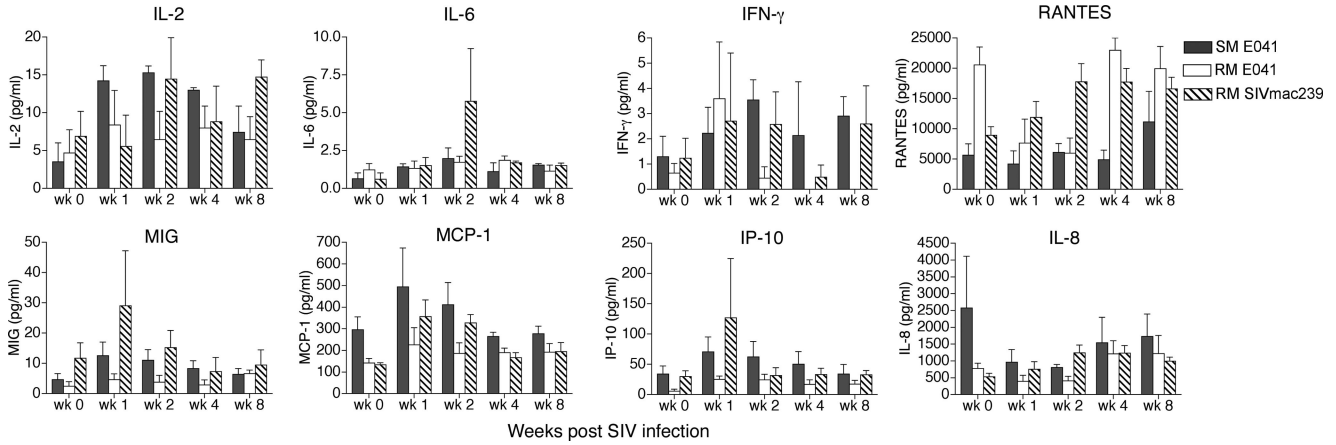

FIG. 8. Kinetics of plasma cytokines and chemokines after SIV infection in SM and RM. Means and standard errors of the means of data for four SIVsmE041-infected SM, four SIVsmE041-infected RM, and six SIVmac239-infected RM are shown. Measurements were made using the cytometric bead array system.

TABLE 1. Plasma cytokine and chemokine levels at week 2 after SIV infection

Animal species (virus)	*n*	Mean pg/ml ± SEM							
		IL-2	IL-6	IFN-γ	RANTES	MIG	MCP-1	IP-10	IL-8
SM (SIVsmE041)	4	15.2 ± 0.9	1.9 ± 0.7	3.5 ± 0.79	6,100 ± 1469	11 ± 3.5	411.6 ± 102	62.3 ± 25.3	802 ± 94.7
RM (SIVmac239)	6	14.4 ± 5.4	5.7 ± 3.4	2.5 ± 1.2	17,763 ± 2999	15.2 ± 5.6	327 ± 38	31.6 ± 12.9	1,241 ± 229
P value[a]		0.9	0.41	0.58	**0.01**	0.59	0.39	0.26	0.17

[a] Determined by the two-tailed unpaired *t* test. Detection limits of the cytometric bead array were as follows: IL-2, 0.6 pg/ml; IL-6, 0.1 pg/ml; IFN-γ, 3.3 pg/ml; IL-8, 0.2 pg/ml; RANTES, 1.0 pg/ml; MIG, 2.5 pg/ml; MCP-1, 2.7 pg/ml; IP-10, 2.8 pg/ml.

observed in the peripheral blood but not the LNs during acute SIV infection.

The relative absence of $CD4^+$ T-lymphocyte activation and apoptosis in SM during acute SIV infection could be due to the presence of fewer productively infected $CD4^+$ T lymphocytes, resulting in less direct cell death, or it could be due to limited activation of uninfected, bystander T lymphocytes, resulting in less indirect cell death. There are currently no data on the number of SIV-infected $CD4^+$ T lymphocytes during acute SIV infection in natural hosts. In RM, 30 to 60% of memory $CD4^+$ T lymphocytes are infected in the first 2 weeks after SIV infection and implicated in the loss of $CD4^+$ T lymphocytes in acute SIV infection (22). Natural hosts also develop profound depletion of gut $CD4^+$ T lymphocytes during acute SIV infection (12, 29). If this loss is also primarily due to direct cell death, it would suggest that natural and nonnatural hosts may not differ substantially with regard to the number of productively infected $CD4^+$ T lymphocytes in acute SIV infection. In this study, we did not find evidence to support a link between ex vivo $CD4^+$ T-lymphocyte apoptosis and the number of productively infected $CD4^+$ T lymphocytes. Thus, plasma SIV RNA at the height of viral replication did not correlate with $CD4^+$ T-lymphocyte apoptosis. SIVsmE041-infected SM had peak viremia levels similar to or higher than those in SIVsmE041-infected RM but did not show increased $CD4^+$ T-lymphocyte apoptosis, whereas SIVsmE041- and SIVmac239-infected RM had a 1-log-unit or greater difference in levels of peak viremia but a similar magnitude of $CD4^+$ T-lymphocyte apoptosis. Since the plasma viral load in acute SIV infection in RM directly correlates with the number of SIV-infected $CD4^+$ T lymphocytes in the peripheral blood (22), these data suggest that differences in apoptosis of $CD4^+$ T lymphocytes between SM and RM are unlikely to be due to differences in the magnitude of direct cell death. Instead, species-specific differences in susceptibility to SIV-related mechanisms of indirect cell death may be instrumental in the differential T-lymphocyte apoptosis of RM and SM $CD4^+$ T lymphocytes in acute SIV infection. One possibility is that RM $CD4^+$ T lymphocytes are more susceptible to apoptosis triggered by virion gp120-mediated upregulation of Fas-Fas ligand (20). Alternately, other mechanisms, such as susceptibility to TRAIL-mediated apoptosis as suggested by this study, likely contribute to apoptosis of uninfected $CD4^+$ T lymphocytes in SIV-infected RM. The finding of an early increase in $CD4^+$ T-lymphocyte apoptosis primarily restricted to activated, uninfected bystander T lymphocytes is consistent with other studies of acute SIV infection (9, 20). The nature of the double-negative T lymphocytes undergoing apoptosis is not clear. In vitro SIV-infected macaque $CD4^+$ T lymphocytes show marked downmodulation of surface CD4 expression (M. Meythaler and A. Kaur, unpublished data). Thus, in addition to nonspecific activation, some of the apoptotic double-negative T lymphocytes may represent SIV-infected $CD4^+$ T lymphocytes with low to absent surface CD4 expression.

Increased T-lymphocyte activation was observed in the acute phase of SIV infection in SIVsmE041-infected SM but appeared to be restricted primarily to virus-specific $CD8^+$ T lymphocytes that emerged in response to SIV infection. A rapid expansion and contraction phase of SIV-specific $CD8^+$ T lymphocytes was observed in both SM and RM as manifested by detection of the SIV-specific cellular immune response in conjunction with a rapid increase in $CD8^+$ T-lymphocyte proliferation and apoptosis. Interestingly, the magnitude of the SIV-specific IFN-γ ELISPOT response did not differ in the two species, a finding consistent with our previous observation in chronic SIV infection (33). However, the increase in Ki67-positive $CD8^+$ T lymphocytes in the first 6 weeks was significantly higher in the SIV-infected RM than in the SIV-infected SM. These findings raise the possibility that RM may be responding to SIV infection with expansion and activation of virus-specific and non-virus-specific bystander T lymphocytes, whereas SM respond primarily with activation of virus-specific T lymphocytes. Since quantitative estimates of SIV-specific T lymphocytes in the current study were based on enumeration of IFN-γ-secreting cells, we cannot exclude the possibility that the majority of "excess" Ki67-positive $CD8^+$ T lymphocytes in SIV-infected RM are virus-specific cells displaying other effector functions. Our previous data showing qualitative similarities in the SIV-specific cellular immune responses mounted by SM and RM make this less likely (33). By successfully managing to focus the acute response toward SIV-specific immunity, natural hosts could avoid initiation of chronic aberrant immune activation. If so, the limited activation of uninfected and non-virus-specific T lymphocytes in SM from the onset of SIV infection is likely to be due to species-specific differences in the innate immune response to SIV in SM and RM.

What differences in the early innate immune response might result in differential immune activation in the two species? The increase in proinflammatory cytokines and chemokines indicated similarities in the early innate response to SIV in both species. The increase in plasma TRAIL in SIV-infected RM but not SIV-infected SM suggested that the type I interferon responses to SIV infection, particularly that of IFN-α, were different in the two species. IFN-α is a crucial component of the innate immune response that is produced chiefly by plas-

macytoid dendritic cells (pDCs) and serves as an important link between innate and adaptive immunity against viral infections (4). In vitro studies have shown that HIV activates pDCs to increase IFN-α production, which in turn upregulates the expression of TRAIL in monocytes and the expression of death receptors DR-5 on $CD4^+$ T lymphocytes (1, 14, 15). This mechanism is thought to be responsible for the increased susceptibility to $CD4^+$ T-lymphocyte apoptosis in progressor HIV-infected humans and for resistance against $CD4^+$ T-lymphocyte apoptosis in nonprogressors and natural hosts (16, 19). An IFN-α-independent, Tat-dependent increase in TRAIL has also been described (19, 34). The present study is the first to longitudinally measure plasma levels of TRAIL in a nonnatural host and a natural host from the onset of SIV infection. Our finding of increased plasma TRAIL and increased $CD4^+$ T-lymphocyte apoptosis, along with their direct association in SIV-infected RM but not SIV-infected SM, is consistent with TRAIL-mediated apoptosis of predominantly uninfected, bystander $CD4^+$ T lymphocytes being a mechanism of $CD4^+$ T-cell death in pathogenic infection (34). Of interest, an early increase in plasma soluble TRAIL levels occurring around the viral ramp-up phase was recently reported as a feature of acute HIV type 1 infection (10). We were not able to establish a definite link between increased TRAIL and increased IFN-α production in SIV-infected RM. Even though there was a positive correlation between the two parameters, increased TRAIL was observed in all SIV-infected RM, but an increase in plasma IFN-α was detected in only a subset of SIVmac239-infected macaques with high levels of peak viremia. Whether this reflects poor sensitivity of the IFN-α ELISA, missing the time point of peak IFN-α increase, or IFN-α-independent increased TRAIL production remains to be determined. From the current study, we cannot ascertain whether the lack of increased TRAIL production and $CD4^+$ T-lymphocyte apoptosis in SIV-infected SM was due to impaired IFN-α production by SM pDCs. A recent report of increased plasma IFN-α in AGM after SIV inoculation suggests that pDCs of natural hosts are not defective for IFN-α production (6).

Whether the acute increase in plasma TRAIL and apoptosis of $CD4^+$ and double-negative T lymphocytes are predictive of disease outcome in SIV-infected RM remains to be determined. It should be noted that even though SIVsmE041 infection was controlled in RM, the ultimate outcome is unlikely to be nonpathogenic. The initial control of viremia in SIVsmE041-infected RM is consistent with the slow disease progression and viremia levels seen after infection of RM with nonadapted primary SIVsm isolates (11). However, such RM invariably progress to AIDS, although over a longer duration (C. Apetrei, personal communication), and thus it is unlikely that SIVsmE041 infection is nonpathogenic in RM. Studies with live attenuated strains of SIV, or following acute viral infections other than SIV, will shed better light on the relationship between early TRAIL induction and development of AIDS in SIV-infected RM.

In summary, an early proinflammatory cytokine and chemokine response accompanied by onset of virus-specific cellular immunity suggests common pathways in the innate and adaptive immune responses to SIV in RM and SM. Differences in $CD4^+$ T-lymphocyte apoptosis and TRAIL induction indicate as-yet-unknown differences in the innate immune response that lead to a more controlled virus-focused response in SM but to a more diffuse response attended by collateral damage in RM. The points of similarity and divergence in the early host response to SIV in SM and RM revealed in this study have implications for understanding the basis for nonpathogenic infection in natural hosts.

ACKNOWLEDGMENTS

This work was supported by Public Health Service grants RR00168, RR00165, AI49809, and AI46006. Work by the Emory University CFAR virology core was supported by Emory CFAR Center grant P30 AI50409.

We thank Michael Piatak, Jr., and Jeffrey Lifson at the SAIC Frederick AIDS vaccine program for the determination of the SIVmac239 viral loads and the Emory University CFAR virology core for the SIVsmE041 RNA measurements.

REFERENCES

1. **Audige, A., M. Urosevic, E. Schlaepfer, R. Walker, D. Powell, S. Hallenberger, H. Joller, H. U. Simon, R. Dummer, and R. F. Speck.** 2006. Anti-HIV state but not apoptosis depends on IFN signature in CD4+ T cells. J. Immunol. **177:**6227–6237.
2. **Chakrabarti, L. A., S. R. Lewin, L. Zhang, A. Gettie, A. Luckay, L. N. Martin, E. Skulsky, D. D. Ho, C. Cheng-Mayer, and P. A. Marx.** 2000. Normal T-cell turnover in sooty mangabeys harboring active simian immunodeficiency virus infection. J. Virol. **74:**1209–1223.
3. **Cline, A. N., J. W. Bess, M. Piatak, Jr., and J. D. Lifson.** 2005. Highly sensitive SIV plasma viral load assay: practical considerations, realistic performance expectations, and application to reverse engineering of vaccines for AIDS. J. Med. Primatol **34:**303–312.
4. **Colonna, M., G. Trinchieri, and Y. J. Liu.** 2004. Plasmacytoid dendritic cells in immunity. Nat. Immunol. **5:**1219–1226.
5. **Cumont, M. C., O. Diop, B. Vaslin, C. Elbim, L. Viollet, V. Monceaux, S. Lay, G. Silvestri, R. Le Grand, M. Muller-Trutwin, B. Hurtrel, and J. Estaquier.** 2008. Early divergence in lymphoid tissue apoptosis between pathogenic and nonpathogenic simian immunodeficiency virus infections of nonhuman primates. J. Virol. **82:**1175–1184.
6. **Diop, O. M., M. J. Ploquin, L. Mortara, A. Faye, B. Jacquelin, D. Kunkel, P. Lebon, C. Butor, A. Hosmalin, F. Barre-Sinoussi, and M. C. Muller-Trutwin.** 2008. Plasmacytoid dendritic cell dynamics and alpha interferon production during simian immunodeficiency virus infection with a nonpathogenic outcome. J. Virol. **82:**5145–5152.
7. **Estaquier, J., T. Idziorek, F. de Bels, F. Barre-Sinoussi, B. Hurtrel, A. M. Aubertin, A. Venet, M. Mehtali, E. Muchmore, P. Michel, Y. Mouton, M. Girard, and J. C. Ameisen.** 1994. Programmed cell death and AIDS: significance of T-cell apoptosis in pathogenic and nonpathogenic primate lentiviral infections. Proc. Natl. Acad. Sci. USA **91:**9431–9435.
8. **Estes, J. D., S. N. Gordon, M. Zeng, A. M. Chahroudi, R. M. Dunham, S. I. Staprans, C. S. Reilly, G. Silvestri, and A. T. Haase.** 2008. Early resolution of acute immune activation and induction of PD-1 in SIV-infected sooty mangabeys distinguishes nonpathogenic from pathogenic infection in rhesus macaques. J. Immunol. **180:**6798–6807.
9. **Finkel, T. H., G. Tudor-Williams, N. K. Banda, M. F. Cotton, T. Curiel, C. Monks, T. W. Baba, R. M. Ruprecht, and A. Kupfer.** 1995. Apoptosis occurs predominantly in bystander cells and not in productively infected cells of HIV- and SIV-infected lymph nodes. Nat. Med. **1:**129–134.
10. **Gasper-Smith, N., D. M. Crossman, J. F. Whitesides, N. Mensali, J. S. Ottinger, S. G. Plonk, M. A. Moody, G. Ferrari, K. J. Weinhold, S. E. Miller, C. F. Reich III, L. Qin, S. G. Self, G. M. Shaw, T. N. Denny, L. E. Jones, D. S. Pisetsky, and B. F. Haynes.** 2008. Induction of plasma (TRAIL), TNFR-2, Fas ligand, and plasma microparticles after human immunodeficiency virus type 1 (HIV-1) transmission: implications for HIV-1 vaccine design. J. Virol. **82:**7700–7710.
11. **Gautam, R., A. C. Carter, N. Katz, I. F. Butler, M. Barnes, A. Hasegawa, M. Ratterree, G. Silvestri, P. A. Marx, V. M. Hirsch, I. Pandrea, and C. Apetrei.** 2007. In vitro characterization of primary SIVsmm isolates belonging to different lineages. In vitro growth on rhesus macaque cells is not predictive for in vivo replication in rhesus macaques. Virology **362:**257–270.
12. **Gordon, S. N., N. R. Klatt, S. E. Bosinger, J. M. Brenchley, J. M. Milush, J. C. Engram, R. M. Dunham, M. Paiardini, S. Klucking, A. Danesh, E. A. Strobert, C. Apetrei, I. V. Pandrea, D. Kelvin, D. C. Douek, S. I. Staprans, D. L. Sodora, and G. Silvestri.** 2007. Severe depletion of mucosal CD4+ T cells in AIDS-free simian immunodeficiency virus-infected sooty mangabeys. J. Immunol. **179:**3026–3034.
13. **Groux, H., G. Torpier, D. Monte, Y. Mouton, A. Capron, and J. C. Ameisen.** 1992. Activation-induced death by apoptosis in CD4+ T cells from human immunodeficiency virus-infected asymptomatic individuals. J. Exp. Med. **175:**331–340.

14. **Herbeuval, J. P., A. Boasso, J. C. Grivel, A. W. Hardy, S. A. Anderson, M. J. Dolan, C. Chougnet, J. D. Lifson, and G. M. Shearer.** 2005. TNF-related apoptosis-inducing ligand (TRAIL) in HIV-1-infected patients and its in vitro production by antigen-presenting cells. Blood **105:**2458–2464.
15. **Herbeuval, J. P., J. C. Grivel, A. Boasso, A. W. Hardy, C. Chougnet, M. J. Dolan, H. Yagita, J. D. Lifson, and G. M. Shearer.** 2005. CD4+ T-cell death induced by infectious and noninfectious HIV-1: role of type 1 interferon-dependent, TRAIL/DR5-mediated apoptosis. Blood. **106:**3524–3531.
16. **Herbeuval, J. P., J. Nilsson, A. Boasso, A. W. Hardy, M. J. Kruhlak, S. A. Anderson, M. J. Dolan, M. Dy, J. Andersson, and G. M. Shearer.** 2006. Differential expression of IFN-alpha and TRAIL/DR5 in lymphoid tissue of progressor versus nonprogressor HIV-1-infected patients. Proc. Natl. Acad. Sci. USA **103:**7000–7005.
17. **Kaur, A., M. Di Mascio, A. Barabasz, M. Rosenzweig, H. M. McClure, A. S. Perelson, R. M. Ribeiro, and R. P. Johnson.** 2008. Dynamics of T- and B-lymphocyte turnover in a natural host of simian immunodeficiency virus. J. Virol. **82:**1084–1093.
18. **Kaur, A., R. M. Grant, R. E. Means, H. McClure, M. Feinberg, and R. P. Johnson.** 1998. Diverse host responses and outcomes following simian immunodeficiency virus SIVmac239 infection in sooty mangabeys and rhesus macaques. J. Virol. **72:**9597–9611.
19. **Kim, N., A. Dabrowska, R. G. Jenner, and A. Aldovini.** 2007. Human and simian immunodeficiency virus-mediated upregulation of the apoptotic factor TRAIL occurs in antigen-presenting cells from AIDS-susceptible but not from AIDS-resistant species. J. Virol. **81:**7584–7597.
20. **Li, Q., L. Duan, J. D. Estes, Z. M. Ma, T. Rourke, Y. Wang, C. Reilly, J. Carlis, C. J. Miller, and A. T. Haase.** 2005. Peak SIV replication in resting memory CD4+ T cells depletes gut lamina propria CD4+ T cells. Nature **434:**1148–1152.
21. **Ling, B., C. Apetrei, I. Pandrea, R. S. Veazey, A. A. Lackner, B. Gormus, and P. A. Marx.** 2004. Classic AIDS in a sooty mangabey after an 18-year natural infection. J. Virol. **78:**8902–8908.
22. **Mattapallil, J. J., D. C. Douek, B. Hill, Y. Nishimura, M. Martin, and M. Roederer.** 2005. Massive infection and loss of memory CD4+ T cells in multiple tissues during acute SIV infection. Nature **434:**1093–1097.
23. **Meyaard, L., S. A. Otto, R. R. Jonker, M. J. Mijnster, R. P. Keet, and F. Miedema.** 1992. Programmed death of T cells in HIV-1 infection. Science **257:**217–219.
24. **Monceaux, V., J. Estaquier, M. Fevrier, M. C. Cumont, Y. Riviere, A. M. Aubertin, J. C. Ameisen, and B. Hurtrel.** 2003. Extensive apoptosis in lymphoid organs during primary SIV infection predicts rapid progression towards AIDS. AIDS **17:**1585–1596.
25. **Murali-Krishna, K., J. D. Altman, M. Suresh, D. Sourdive, A. Zajac, and R. Ahmed.** 1998. In vivo dynamics of anti-viral CD8 T cell responses to different epitopes. An evaluation of bystander activation in primary and secondary responses to viral infection. Adv. Exp. Med. Biol. **452:**123–142.
26. **National Research Council.** 1996. Guide for care and use of laboratory animals, p.86–123. National Academy Press, Washington, DC.
27. **Novembre, F. J., J. De Rosayro, S. P. O'Neil, D. C. Anderson, S. A. Klumpp, and H. M. McClure.** 1998. Isolation and characterization of a neuropathogenic simian immunodeficiency virus derived from a sooty mangabey. J. Virol. **72:**8841–8851.
28. **O'Neil, S. P., C. Suwyn, D. C. Anderson, G. Niedziela, J. Bradley, F. J. Novembre, J. G. Herndon, and H. M. McClure.** 2004. Correlation of acute humoral response with brain virus burden and survival time in pig-tailed macaques infected with the neurovirulent simian immunodeficiency virus SIVsmmFGb. Am. J. Pathol. **164:**1157–1172.
29. **Pandrea, I. V., R. Gautam, R. M. Ribeiro, J. M. Brenchley, I. F. Butler, M. Pattison, T. Rasmussen, P. A. Marx, G. Silvestri, A. A. Lackner, A. S. Perelson, D. C. Douek, R. S. Veazey, and C. Apetrei.** 2007. Acute loss of intestinal CD4+ T cells is not predictive of simian immunodeficiency virus virulence. J. Immunol. **179:**3035–3046.
30. **Rey-Cuille, M. A., J. L. Berthier, M. C. Bomsel-Demontoy, Y. Chaduc, L. Montagnier, A. G. Hovanessian, and L. A. Chakrabarti.** 1998. Simian immunodeficiency virus replicates to high levels in sooty mangabeys without inducing disease. J. Virol. **72:**3872–3886.
31. **Silvestri, G., D. L. Sodora, R. A. Koup, M. Paiardini, S. P. O'Neil, H. M. McClure, S. I. Staprans, and M. B. Feinberg.** 2003. Nonpathogenic SIV infection of sooty mangabeys is characterized by limited bystander immunopathology despite chronic high-level viremia. Immunity **18:**441–452.
32. **Viollet, L., V. Monceaux, F. Petit, R. Ho Tsong Fang, M. C. Cumont, B. Hurtrel, and J. Estaquier.** 2006. Death of CD4+ T cells from lymph nodes during primary SIVmac251 infection predicts the rate of AIDS progression. J. Immunol. **177:**6685–6694.
33. **Wang, Z., B. Metcalf, R. M. Ribeiro, H. McClure, and A. Kaur.** 2006. Th-1-type cytotoxic $CD8^+$ T-lymphocyte responses to simian immunodeficiency virus (SIV) are a consistent feature of natural SIV infection in sooty mangabeys. J. Virol. **80:**2771–2783.
34. **Yang, Y., I. Tikhonov, T. J. Ruckwardt, M. Djavani, J. C. Zapata, C. D. Pauza, and M. S. Salvato.** 2003. Monocytes treated with human immunodeficiency virus Tat kill uninfected $CD4^+$ cells by a tumor necrosis factor-related apoptosis-induced ligand-mediated mechanism. J. Virol. **77:**6700–6708.